Immobilization of Growth Factors on Collagen Scaffolds Mediated by Polyanionic Collagen Mimetic Peptides and Its Effect on Endothelial Cell Morphogenesis

Allen Y. Wang,[†] Shirley Leong,[‡] Yu-Chuan Liang,[§] Ru Chih C. Huang,[§] Christopher S. Chen,[||] and S. Michael Yu*[,†,‡]

Department of Materials Science and Engineering, Department of Chemical and Biomolecular Engineering, and Department of Biology, The Johns Hopkins University, Baltimore, Maryland 21218, and Department of Bioengineering, University of Pennsylvania, Philadelphia, Pennsylvania 19104

Received July 2, 2008; Revised Manuscript Received August 6, 2008

Angiogenesis, a morphogenic event endothelial cells (ECs) undergo in response to 3-D environmental triggers, is critical to the survival and ultimate functional capacity of engineered tissue constructs. Here we present a new collagen mimetic peptide (CMP) architecture consisting of multiple anionic charges at the peptide's N-terminus designed to attract growth factors by charge−charge interactions and bind to collagen by CMP−collagen interaction. The anionic CMPs exhibited specific binding affinity to type I collagen substrates while attracting vascular endothelial growth factors (VEGFs), which led to enhanced morphological features of ECs, indicative of tubulogenesis. The results show that these new CMPs could be used to direct proliferation and differentiation of cells in collagen scaffolds by localization and sustained delivery of growth factors and other morphogens.

Introduction

One of the critical design-limiting steps that determines the survival and ultimate functional capacity of engineered tissue constructs centers around their successful vascularization.[1] Based on the rate of oxygen consumption and its diffusion rate through tissue, it is estimated that many parenchymal cells must remain within 200 μm of the nearest capillary to function optimally.[2,3] This vascular constraint can severely limit the size and architecture of 3-D cellular constructs, resulting in an urgent need to induce and control angiogenesis inside these constructs. Through recent studies, we are beginning to understand how various growth factors cooperate with components of the extraceullar matrix (ECM) such as collagen, laminin, fibrin, and other glycoproteins to regulate microvasculature formation;[4−6] however, we are far from creating functional vasculature systems at the speed and level of organization exemplified by natural tissues.[7,8]

Angiogenesis involves the migration, proliferation, and differentiation of endothelial cells (ECs), which are the main cellular components of blood vessel walls. During the active process of angiogenesis, endothelial cells are stimulated by angiogenic factors to degrade the pre-existing ECM and migrate into tissues surrounding an existing blood vessel, where they proliferate and form tube-like structures that branch out to neighboring vessels.[9] Lumen formation then occurs to hollow out the new tubes, completing the formation of the new blood vessel network.[10−12]

Research has shown that vascular endothelial growth factor (VEGF) is an essential factor for the development, proliferation, and maintenance of healthy vasculature.[13] In mammals, the VEGF family is composed of five members including VEGF-A, VEGF-B, VEGF-C, VEGF-D, and PIGF (placenta growth factor). Among them, human VEGF-A with four different isoforms with varying affinity to heparin is believed to be a key regulator of blood vessel growth that controls the balance between new capillary growth and branching.[14−19]

When VEGF is introduced into a host environment, it has a half-life of around 90 min. If the VEGF signal is removed, vessel formation starts to decrease. These findings prompted a number of research groups to develop sustained VEGF delivery systems. Some examples include a polymeric system composed of poly(lactide-*co*-glycolide) and alginate to provide a sustained and localized level of VEGF for angiogenesis and bone regeneration,[20−23] a PEG-cross-linked heparin gel for sustained release of VEGF,[6] immobilization of $VEGF_{165}$ onto a negatively charged poly(tetrafluoroethylene) (PTFE) surface,[24] or a totally synthetic bioactive hydrogel that is able to deliver VEGF when triggered by collagenase (MMP-2).[25,26] Although a variety of synthetic and biologically derived materials have been explored as artificial scaffolds for vasculature engineering, only natural scaffolds such as collagen and fibrin have produced blood vessels that are structurally and functionally equivalent to natural ones.[27]

Collagen, the most abundant protein in mammals and a major component of the ECM, induces proliferation and differentiation of cells through direct binding interactions and by serving as a reservoir for growth factors and signaling molecules. Furthermore, it provides a structural framework during tissue development and repair. Due to its abundance, collagens (especially type I and II collagen) can be readily isolated from animal tissues, stored in solution or as a solid, and used as biocompatible coatings or soft-tissue substitutes that can protect and support damaged tissues.[28] Lately, 2-D and 3-D collagen constructs have been widely used as tissue scaffolds in a variety of applications, including skin replacement, bone substitution, and artificial blood vessels and valves.[29]

Scientists have attempted to insert a number of different therapeutic compounds into collagens to facilitate tissue regen-

* To whom correspondence should be addressed. E-mail: yu@jhu.edu.
[†] Department of Materials Science and Engineering.
[‡] Department of Chemical and Biomolecular Engineering.
[§] Department of Biology.
[||] Department of Bioengineering.

10.1021/bm800727z CCC: $40.75
Published on Web 09/25/2008

eration.[30] A collagen-glycosaminoglycan (GAG) analogue was successfully used for nerve and dermal regeneration as well as promoting angiogenesis in vivo,[31−33] while human umbilical vascular endothelial cells (HUVECs) exhibited significant angiogenesis when cultured in scaffolds comprising both type I collagen and sulfated GAGs.[4] Scientists have also covalently conjugated heparin to collagen substrates for improving blood compatibility and endothelialization of vascular grafts by local release of basic fibroblast growth factor (bFGF).[5,6] In addition, a $VEGF_{121}$ derivative with fibronectin and collagen binding domains was shown to maintain bioactivity in the presence of the collagen matrix and stimulate EC activity,[34] while covalent immobilization of VEGF to collagen matrices using homobifunctional cross-linking agent, NHS-PEG_{3400}-NHS, resulted in positive effects on microvasculature formation both in vitro and in vivo.[35]

Due to the biochemical and structural complexity of the collagens, however, covalent conjugation can be difficult to control, produce poor reaction yields, and even compromise the biochemical features of natural collagens.[35,36] Most importantly, chemical reactions are not ideal for modifying integrated collagen matrices that contain bioactive compounds and live cells because such chemical reactions are not specific to collagens. Therefore, we have explored an alternative noncovalent binding process that is collagen-specific. Such a process can not only evade the drawbacks of chemical modifications,[37] but may allow better spatial control of the modification since it can be applied directly to prefabricated collagen scaffolds.

The triple-helical structure of collagen has fascinated scientists for its unique multiplex architecture and its essential role in formation of functional collagen molecules and their higher order assembly.[38] Collagens are composed of three separate polypeptide strands that are rich in proline (Pro) and hydroxyproline (Hyp), which confer rigidity to the backbone conformation. Periodic repeats of glycine (Gly) at every third residue allow the three collagen strands to pack closely and form a stable triple helix through interchain hydrogen bonds around a common helical axis, similar to the interactions in a DNA double helix. The triple helix can be found in almost all of the 28 collagen types reported to date, as well as in several other noncollagen proteins such as complement proteins and mannose binding proteins.[39]

In an effort to develop a facile collagen modification based on collagen's native ability to associate into triple helical molecular architecture, we investigated the folding behavior of synthetic collagen mimetic peptide (CMP) [$(ProHypGly)_x$; Hyp: hydroxyproline] in contact with natural collagen and discovered CMP's structure-dependent binding affinity to type I collagen.[37,40] The binding experiments indicated that type I collagen fibers attract only single-stranded CMPs, not triple helical CMPs or control peptides with scrambled peptide sequences. CMP seems to be "hitch-hiking" onto natural collagen by forming a CMP−collagen complex stabilized by triple helix assembly. The affinity between single-stranded CMPs and collagen has been used to physically modify purified collagen, for example, to create poly(ethylene glycol)-CMP-collagen substrates that repel cell attachment[37] and poly(ethylene glycol)-CMP-collagen hybrid hydrogel ideal for chondrocyte and mesenchymal stem cell encapsulation.[41,42]

Here we present a new CMP architecture (Figure 1A) consisting of multiple anionic charges at the peptide's N-terminus, designed to bind to collagen scaffolds by strand invasion and at the same time attract growth factors by charge−charge interactions (Figure 1B). Using this CMP, we were able to immobilize high concentrations of VEGF to collagen gel that promoted HUVEC's tube-like morphology indicative of early signs of angiogenesis.

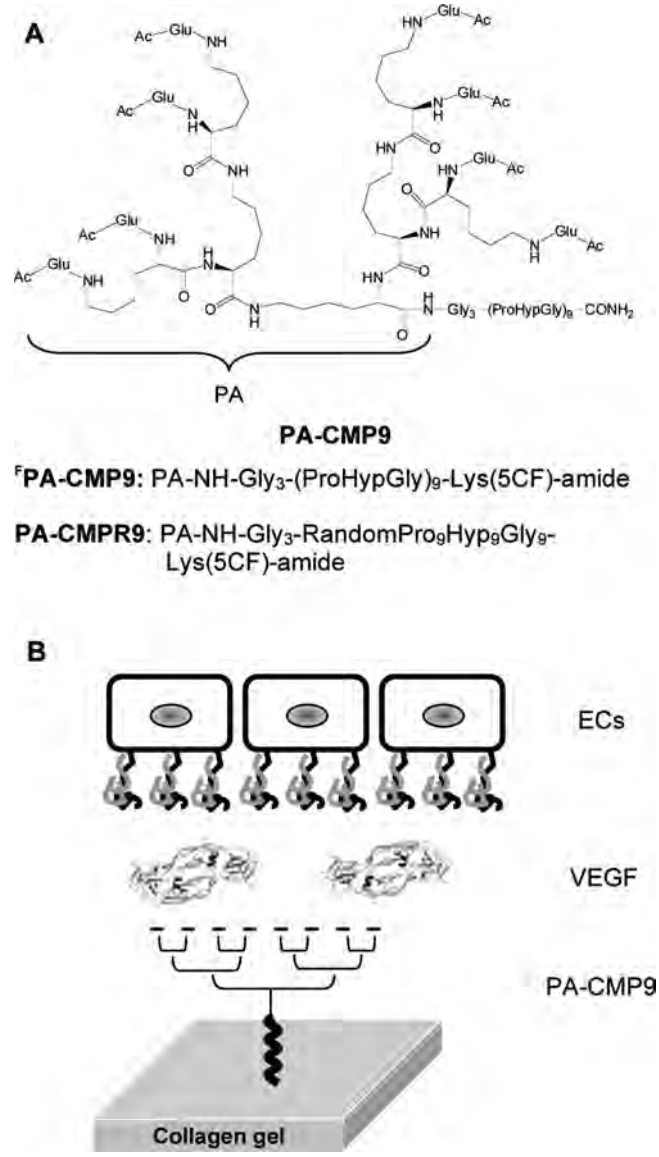

PA-CMP9: PA-NH-Gly_3-$(ProHypGly)_9$-Lys(5CF)-amide

PA-CMPR9: PA-NH-Gly_3-$RandomPro_9Hyp_9Gly_9$-Lys(5CF)-amide

Figure 1. Chemical structures of polyanionic CMPs (A) and schematic of VEGF/**PA-CMP9**/collagen gel construct (B).

Experimental Section

Materials. Fmoc-Gly-OH, Fmoc-Pro-OH, Fmoc-Hyp-OH, Fmoc-Lys(Fmoc)-OH, Fmoc-Glu(OtBu)-OH, Fmoc-Lys(Mmt)-OH, 2-(1*H*-benzo-triazole-1-yl)-1,1,3,3-tetra-methyl uronium hexafluoro phosphate (HBTU), *N*-hydroxybenzotriazole (HOBt), *N*,*N*-diisopropylethylamine (DIPEA), and *N*-methylpyrrolidone (NMP) were purchased from Advanced ChemTech (Louisville, KY). TentaGel S RAM resin was purchased from Rapp-Polymere (Tubingen, Germany). Acid soluble rat-tail type I collagen was purchased from BD Bioscience (San Jose, CA). All other chemicals were purchased from Sigma-Aldrich (St. Louis, MO) or EMD Chemicals Inc. (Gibbstown, NJ) and used without further purification. Human umbilical vein endothelial cells (HUVEC) maintained in EGM medium were obtained from Cambrex (Walkersville, MD). Recombinant human vascular endothelial growth factor $VEGF_{165}$ ($rhVEGF_{165}$) was obtained from Invitrogen Corp. (Carlsbad, CA), while antibodies and reagents for $VEGF_{165}$ assay: (1) primary antibody (rabbit antihuman VEGF antibody, rabbit polyclonal IgG, anti-VEGF); (2) secondary antibody (goat antirabbit IgG conjugate HRP);

(3) tertiary antibody (monoclonal mouse anti-ILK antibody), and (4) protein A/G plus agarose were purchased from Santa Cruz Biotechnology, Inc. (Santa Cruz, CA). Microplates, 96-well MBP (myelin basic protein), and antiphospho-serine/threonine (mixed mouse monoclonal IgGs) were purchased from Upstate Biotechnology Inc. (Temecula, CA). Antimouse IgG conjugate HRP, and recombinant human epidermal growth factor (rhEGF) were obtained from Promega (Madison, WI).

Synthesis of $^{(F)}$PA-CMP9. TentaGel S RAM amide resin (0.2 mmol/g) was swollen in dichloromethane (DCM) and washed in NMP. The resin was treated with corresponding Fmoc-protected amino acid (5.0 equiv), preactivated with activation solution. The activation solution contained 0.25 M HBTU and 0.25 M HOBt in dimethylformamide (DMF). The first amino acid, Fmoc-Gly-OH or Fmoc-Lys(Mmt)-OH, was single-coupled for 10 min followed by double capping with acetic anhydride (0.5 M acetic anhydride containing 0.125 M DIPEA, and 0.015 M HOBt in NMP). This process was used to reduce the resin loading yield and allow only the highly exposed sites on the resin surface to react with the first amino acid.[43] From the second amino acid on, double coupling and double capping methods, each with 30 min reaction time were used. Fmoc deprotection was achieved by treating the resin with 20% piperidine in NMP, and the deprotection reaction was monitored using a conductivity flow cell. The very last capping reaction was repeated four times.

After complete synthesis of the target sequence and final Fmoc deprotection and capping reactions, the resin was washed repeatedly with NMP, DCM, and methanol, and finally dried in vacuum overnight. For the synthesis of **$^{(F)}$PA-CMP9**, the acid-labile 4-monomethoxytrityl (Mmt) was removed by treatment with a mixture of 95% DCM, 4% triisoopropylsilane (TIS), and 1% trifluoroacetic acid (TFA) for 5 min. The procedure was repeated 10 times and followed by DCM wash. The active ε-amine was confirmed with ninhydrin test. To conjugate 5-carboxyfluorescene to the ε-amino group, the resin was first swollen in DCM containing DIPEA and then 5-carboxyfluorescein *N*-succinimidyl ester was added to the reaction mixture. The reaction was allowed to take place for 2−3 days in the dark. The crude peptides were cleaved from resins by treating it with a mixture of 95% TFA, 2.5% TIS, and 2.5% water for 4−6 h. This process also removes the OtBu from the Glu side chain. The crude CMP derivatives were precipitated with cold ether and dried in a vacuum.

Cleaved peptide was purified using semipreparative reverse-phase HPLC on Varian Polaris 210 series liquid chromatograph equipped with a UV detector (wavelength: 220 or 493 nm) and a Vydac C-18 reverse-phase column (Grace, Deerfield, IL) at a flow rate of 4 mL/min. The lyophilized peptide was analyzed by a matrix-assisted laser desorption/ionization time-of-flight (MALDI-TOF) mass spectrometer (Voyager DE-STR, Applied Biosystems, Foster City, CA). **PA-CMP9** $[M + H]^+ = 4849.5$ Da (calcd = 4847.5 Da); **$^{(F)}$PA-CMP9** $[M + K + H]^+ = 5353.4$ Da (calcd = 5313.3 Da); **PA-CMPR9** $[M + H]^+ = 4849.5$ Da (calcd = 4847.5 Da); **CMP9** $[M + H]^+ = 2593.9$ Da (calcd = 2593.0 Da).

Circular Dichroism Thermal Melting Temperature Measurements. Circular dichroism (CD) spectra were recorded on a JASCO 710 spectrometer equipped with JASCO PTC-348 WI temperature controller and Hellma cell (400 μL, 0.1 mm path length). The thermal melting curves were obtained by measuring the molar ellipticity at 225 nm with 1 °C/min heating rate and all samples (100 μM in pH 7.4 PBS) were equilibrated at 4 °C for 24 h before the CD measurement. The concentrations of peptides were determined by UV−vis spectrophotometer at 214 or 493 nm.[44,45] Midpoint (or inflection point) of the sigmoidal melting curve was taken as the melting temperature, T_m.

Determination of Refolding Yields of $^{(F)}$PA-CMP9. The refolding yields of **PA-CMP9** and **$^{(F)}$PA-CMP9** were determined from the CD spectra by taking the following ratio: refolding yield = [helical content of quenched sample]/[helical content of fully folded sample] = [signal A − signal C]/[signal B − signal C], where A = CD intensity (at 225 nm) after quenching from 80 to 25 °C within 4 min, B = CD intensity (at 225 nm) after overnight incubation at 10 °C, and C = CD intensity (at 225 nm) after 3 h incubation incubated at 80 °C.

Preparation of Collagen Gel. Reconstituted type I collagen solution (30 mL, 3 mg/mL) was prepared by mixing 23.75 mL of cold type I rat tail collagen solution (3.79 mg/mL in 0.012 N HCl solution) and cold reconstituted buffer (3 mL sterile 10× phosphate buffered saline, 0.55 mL sterile 1 N NaOH, 2.74 mL sterile H_2O) on ice. Then, 200 or 800 μL of the reconstituted collagen solution was added to each well of 48-well or 12-well culture plates, respectively, and immediately incubated at 37 °C for at least 1 h to allow gel formation.

$^{(F)}$PA-CMP-Modified Collagen Gel. A 100 μL of 100 μM **$^{(F)}$PA-CMP9** solution in PBS pre-equilibriated at 80 °C (designated as **h$^{(F)}$PA-CMP9**) was applied to the collagen gel in 48-well culture plates at room temperature. The gel was left at room temperature for 3 h for binding and subsequently washed with 4 °C PBS (total volume 10 mL). Amount of **$^{(F)}$PA-CMP9** remaining on the collagen gel (initial loading) was determined by measuring the UV−vis absorbance (493 nm) of the wash solutions. For the release experiment, the well was charged with 500 μL of PBS buffer and incubated at 37 °C (5% CO_2). During the incubation, the concentrations of **$^{(F)}$PA-CMP9** released were determined daily by measuring the supernatant's absorbance at 493 nm. The wells were charged with fresh buffer after the absorbance measurements. Data were collected from four independent experiments.

PA-CMP/VEGF-Modified Collagen Gel. In 48-well culture plate, **PA-CMP9**-modified collagen gel was prepared as above. To the well was added VEGF solution in PBS (100 μL, 1 μg/mL) and the culture plate was incubated overnight at 4 °C followed by extensive washing with 4 °C PBS. Amount of VEGF remaining after the wash was determined by the VEGF assay described below. For VEGF release experiment, the well was charged with 500 μL of PBS buffer and incubated at 37 °C (5% CO_2). During the incubation, the concentration of VEGF associated with collagen gel was determined daily by the VEGF assay. Data were collected from four independent experiments.

VEGF Assay. A 200 μL solution of 5% bovine serum albumin (BSA) in PBS-Tween (PBS-T) buffer was added to each well containing **PA-CMP**/VEGF-modified collagen gel and left overnight at 4 °C to block excess reactive sites. The plate was blotted by tapping it upside down on tissue paper and washed three times with 200 μL/well of cold PBST. To each well, a 100 μL solution of anti-VEGF antibody (0.4 μg/mL) was added and the plate was incubated overnight at 4 °C. The washing procedure was then repeated three times with cold PBS-T. The secondary antibody, goat antirabbit IgG conjugate HRP, was diluted in cold PBS-T buffer to 1/1500. To each well, 100 μL of cold dilute secondary antibody solution was added. The plate was incubated at 4 °C for 3 h and then washed with cold PBS-T three times. To each well, 100 μL of HRP substrate solution (9 mL of ABTS, 2,2-azino-di-[3-ethylbenzthiazoline-6-sulfonic acid] and 1 mL of hydrogen peroxide) was added. The plate was gently shaken for 10 min during color development. The resulting fluorescence supernatant was transferred to a 96-well culture dish and its absorbance at 415 nm was determined using a 96-well microplate reader.[46] A standard curve was generated using 0.05, 0.2, 0.4, 0.5, and 0.8 μg of VEGF per well on a 96-well culture plate. For background subtraction, VEGF assay was also performed on unmodified collagen gel. Data were collected from four independent experiments.

HUVEC Morphogenesis on PA-CMP9-Modified Collagen Gel. Collagen gels with **PA-CMP9**/VEGF or **PA-CMPR9**/VEGF modification were seeded with HUVECs (1.5×10^3 cells/well) in 48-well culture plate and incubated at 37 °C for 1 day in EGM (500 μL/well). For control experiments, EGF in PBS (1 μg/mL, pH 7.4) was applied to **PA-CMP9**-modified collagen gel without VEGF addition, followed by HUVEC seeding. The cell morphology was observed using Nikon Eclipse TE2000 optical microscope.

Integrin-Link Kinase (ILK) Assay. HUVECs (passage 6) were cultured on 12-well tissue culture dishes with EGM for 20 h (12×10^3 cells/well). The medium was then removed, and cells were washed twice in PBS. The **PA-CMP9**/VEGF-modified collagen gel was turned

Table 1. Melting Transition Temperatures of Polyanionic Collagen Mimetic Peptides (PA-CMPs) Determined by Circular Dichroism Spectrometer

CMP	T_m[c] (°C)
PA-CMP9[a]	52 ± 1
$^{(F)}$PA-CMP9[a]	54 ± 1
PA-CMPR9[b]	
CMP9	60 ± 1

[a] The structures are shown in Figure 1. [b] CMPR9: GGGPGP^{H}GPGP-P^{H}P^{H}GP^{H}GPP^{H}PGP^{H}P^{H}PGGP^{H}P^{H}PPG-amide, (P^{H}: Hyp). [c] Measured in 57.5 μM, pH 7.4, PBS solution.

upside down and brought in contact with the HUVECs in fresh EGM. After 10 min, the medium and collagen gels were removed from the dishes, and the cells were washed twice with cold PBS. The cells were lysed in 200 μL of cold collagenase PBS solution and sonicated on ice for 5∼10 s. Protein content of the lysates was determined by Bio-Rad protein assay and a total protein of 30 mg was used for the following ILK assay. The lysates were precleaned with protein A/G plus agarose at 4 °C for 1 h. After incubation, the lysates were centrifuged for 10 min at 4 °C. The supernatants were transferred to fresh conical centrifuge tubes on ice and incubated with anti-ILK antibody at 4 °C for 1 day. After incubation, 10 μL of protein A/G plus agarose was added and incubated at 4 °C for 1 h. The immunoprecipitated ILK was collected with protein A/G plus agarose. The pellets from each well were vortexed with 50 μL of kinase reaction buffer (20 mM Hepes, 10 mM $MgCl_2$, 10 mM $MnCl_2$, 2 mM NaF, 1 mM Na_3VO_4, 100 μM ATP) at room temperature for 30 min. The reaction buffer was then added to precoated 96-well MBP microplates. After incubation at room temperature for 1 h, all solutions were removed. A 200 μL solution of 3% BSA in PBS-T buffer was added to each well at 4 °C and incubated for 1 day to block excess reactive sites on the plate. The plate was washed with PBS-T three times and blotted by tapping it upside down on tissue paper. To each well, 200 μL of antiphospho-ser/thr (1:500) was added and the plate was incubated at 4 °C overnight. The plate was washed three times with PBS-T and then dried by tapping it upside down on a tissue paper. Secondary antibody, antimouse IgG conjugated HRP, was diluted to 1:2000 with PBS-T, and 200 μL was added to each well. After incubation at room temperature for 2 h, the plate was washed with PBS-T three times and dried. To each well, 100 μL of HRP substrate solution containing 2,2-azino-di-(3-ethylbenzthiazoline-6-sulfonic acid) and hydrogen peroxide (9:1 respective volume ratio) was added. The plate was gently shaken for 10 min for color development. The resulting fluorescence was measured at 415 nm with a 96-well microplate reader.[46] For control experiments, ILK assay was performed on cells cultured only on culture dish for 20 h (negative control) and on cells that contacted unmodified collagen gel containing 32 ng or 20.5 ng of soluble VEGF (positive control). The two VEGF concentrations correspond respectively to the initial concentrations of VEGF for **hPA-CMP9**- and **qPA-CMP9**-treated collagen gels after 4 °C wash. Data were collected from six independent experiments.

Results and Discussion

Synthesis and Characterization of Polyanionic CMP. We used Fmoc-mediated solid supported peptide synthesis (SSPS) to prepare anionically charged CMP displaying, at its N terminus, a second generation lysine dendrion terminating with eight N-acetylated glutamic acids. The structure of the polyanionic CMP, designated as **PA-CMP9**, is shown in Figure 1 and Table 1. The figure also shows **$^{(F)}$PA-CMP9**, a 5-carboxyfluorescene tagged **PA-CMP9**, and **PA-CMP-R9**, a control peptide with an identical amino acid composition as **PA-CMP9**, but scrambled in sequence and unable to support triple helix formation. Due to the complexity of the molecular structure, **$^{(F)}$PA-CMP9** was synthesized only on a TentaGel S RAM resin.

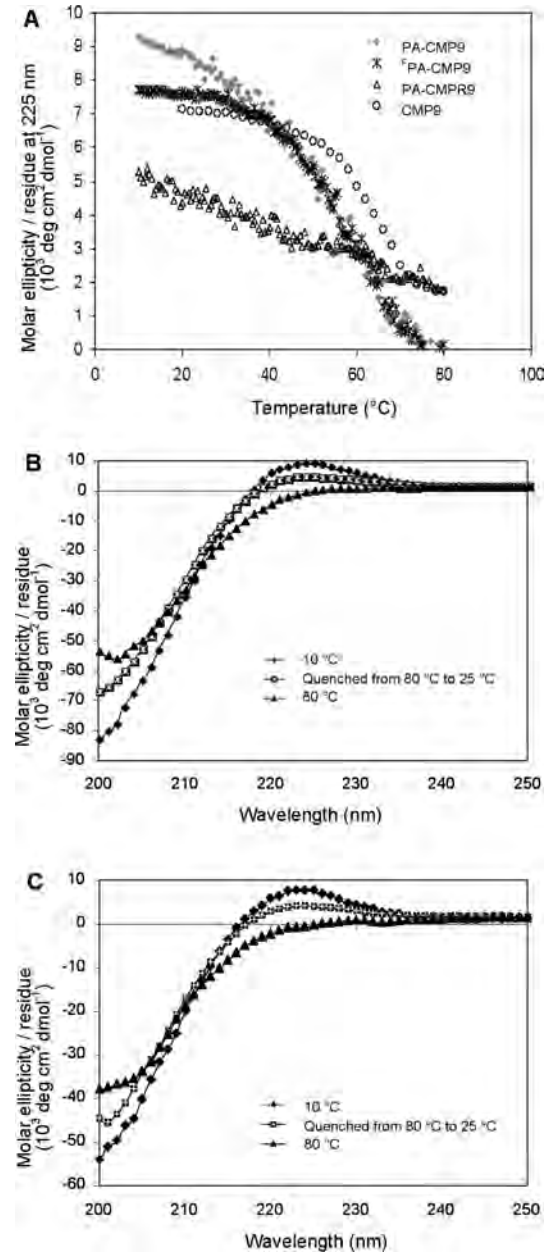

Figure 2. CD melting curves (A) and CD molar ellipticity/residue traces of **PA-CMP9** derivatives (B, **PA-CMP9**; C, **$^{(F)}$PA-CMP9**) measured in PBS buffer (pH 7.4).

Initially, we used Rink amide resin (Novabiochem) as a solid support; however, growth of the peptide chain stopped when Gly_3-$(ProHypGly)_9$ was reached despite many trials under different reaction conditions. When HMBA-PEGA resin (Novabiochem)[47] was used, the peptide chain stopped growing after the first lysine conjugation. TentaGel S RAM, a low-density PEG-supported resin (loading density: 0.2 mmol/g) was used successfully as a solid-support for the **PA-CMP9** synthesis, presumably because of increased accessibility to the growing branched structure for each new amino acid addition.[43]

CD melting curves (Figure 2A and Table 1) indicated that the T_ms of **PA-CMP9** and **$^{(F)}$PA-CMP9** were approximately 52 and 54 °C, respectively, while no melting was observed for **PA-CMPR9**. T_ms are 6−8 °C lower than the corresponding **CMP9** (Table 1), suggesting that the polyanionic dendrion moiety has reduced the thermal stability of the CMP triple helix by steric hindrance and charge−charge repulsion.

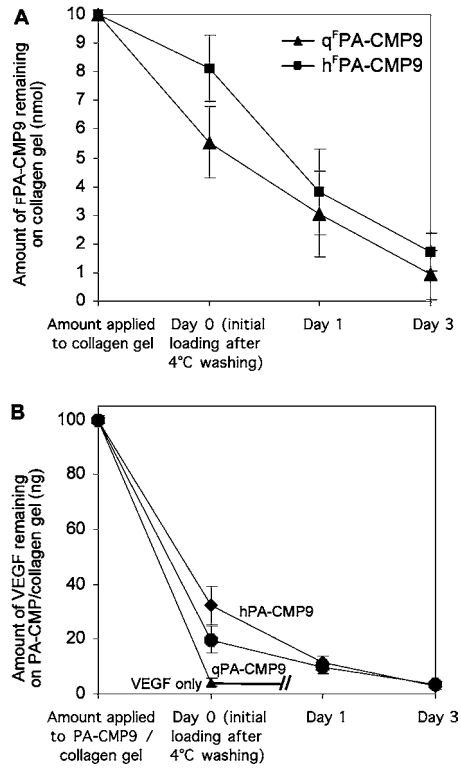

Figure 3. Profiles of **h$^{(F)}$PA-CMP9** and **q$^{(F)}$PA-CMP9** remaining on collagen gels (A), and profiles of VEGF remaining on **PA-CMP9**-treated collagen gel (B) during incubation at 37 °C.

Collagen binding occurs only when melted, single-stranded CMP is allowed to fold in contact with collagen. Previously, we demonstrated such binding affinity by treating type I collagen film with hot CMP solution, and with CMP solution that was quenched from 80 to 25 °C.[47] Binding of quenched CMPs was possible because the folding rates for CMPs with bulky end groups were slow enough that significant portion (30−50%) of CMPs were in single stranded state after quenching. We expected that **PA-CMP9** would also exhibit slow refolding due to the bulky and charged polyanionic unit. Figure 2B,C shows the CD mean residue ellipticity for completely denatured CMP (80 °C solution, bottom curve), fully folded CMP (10 °C solution, top curve), and CMP quenched from 80 to 25 °C in 4 min (middle curve). The refolding yields for **PA-CMP9** and **$^{(F)}$PA-CMP9** solutions (100 μM) were 48.6 and 50.4%, respectively. This indicated that for the quenched **$^{(F)}$PA-CMP9** solution at room temperature, approximately half of the CMPs are in a single-stranded state and available to interact with collagen. Here we designate **$^{(F)}$PA-CMP9** in PBS solution that was preheated at 80 °C as **h$^{(F)}$PA-CMP9** and the one quenched from 80 to 25 °C within 4 min as **q$^{(F)}$PA-CMP9**.

Immobilization of PA-CMPs on Collagen Gel. Type I collagen gel was fabricated by neutralizing and warming the acidic collagen solution (3 mg/mL) in a 48-well culture plate. **h$^{(F)}$PA-CMP9** (80 °C, 100 nmol) was applied to collagen gel sitting at room temperature and the gel was incubated at room temperature for 3 h followed by washing with 4 °C PBS until no fluorescence was detected in the wash solution. Initial binding yield determined from fluorescence of wash solution was 82% after the cold wash (Figure 3A, day 0). When **q$^{(F)}$PA-CMP9** was applied to the collagen gel, the initial binding yield after the cold PBS wash was 55%; this value is close to the percentage of unfolded CMPs (50%) in quenched solution determined by the CD measurement. Therefore, within experimental error, 100% of the unfolded **qPA-CMP9** bound to the collagen gel. The reason that only 82% of the unfolded **hPA-CMP9** bound to the collagen gel is unclear, although such a reduction in binding yield was also observed for collagen films treated with hot CMP solutions.[48] According to previous studies, the amount of CMP that can saturate the binding sites is approximately 225 nmol/cm^2.[46] Therefore, it is unlikely that the lower effective binding yield is the result of binding site saturation. More likely, it is the result of partial denaturation of the collagen gel.

All the **PA-CMP** conjugates exhibited sustained release behavior when incubated in 37 °C PBS solutions (Figure 3A) but to a lesser extent than previously demonstrated for CMP and poly(ethyleneglycole)−CMP conjugates.[48] After 1 day, 3−4 nmol of **$^{(F)}$PA-CMP9** remained associated with the collagen gel, which is significantly lower than the sustainability of CMP without the anionic headgroup.[48] Under similar experimental conditions, less than 70% of fluorescently tagged **CMP7** discharged from collagen in 3 days as compared to 85% for **h$^{(F)}$PA-CMP9** and 90% for **q$^{(F)}$PA-CMP9**. This is another indication that the polyanionic headgroup destabilizes the CMP−collagen interaction. Despite lower sustainability, the **PA-CMP9** induced high local concentration of VEGF and significant improvement in the short term morphogenesis of ECs (see below).

Immobilization of VEGF onto PA-CMP/Collagen Gel System. Collagen gel was prepared in 48-well tissue culture dishes as before and solution of hot or quenched **PA-CMP9** (100 μL of 100 μM in PBS) was added, followed by incubation at room temperature for 3 h, and wash with blank 4 °C PBS. VEGF in PBS (100 μL of 1 μg/mL), corresponding to 100 ng of rhVEGF$_{165}$ per well, was then added. Figure 3B shows the amount of VEGF remaining on unmodified and **PA-CMP9**-modified collagen gels after initial wash and subsequent 37 °C incubation. After extensive 4 °C PBS washing, little (∼4 ng) VEGF was detected on the unmodified collagen gel; in contrast, the **hPA-CMP9**/collagen and **qPA-CMP9**/collagen gel systems contained 32 and 20.5 ng of VEGF, respectively. We believe that such immobilization took place by charge−charge interactions between anionic domain of the **PA-CMP9** and the heparin binding domain of the rhVEGF$_{165}$. According to the **$^{(F)}$PA-CMP9** binding and release study (Figure 3A), the ratio between VEGF and **hPA-CMP9** on collagen gel on day 0 was 3.90 ng/nmol, while the ratio of VEGF to **qPA-CMP9** was 3.77 ng/nmol. After a one-day incubation at 37 °C, 62 and 40% of initial VEGF loading were released from **hPA-CMP9**- and **qPA-CMP9**-modified collagen gel, respectively; however, the ratios of VEGF to **PA-CMP9** on collagen remained at around 3.7 ng/nmol for both systems. This suggests that VEGF and **PA-CMP9** discharged from the collagen gel simultaneously, presumably as a charge−charge complex. Therefore, the immobilization and sustained release of VEGF seems to be dictated by those of the **PA-CMP9**. By employment of CMPs with varying binding affinity to collagen, for example, those with variation in peptide length and composition, one should be able to control the initial loading and subsequent release kinetics of VEGF in collagen scaffolds.[44,48]

Morphogenesis of ECs on PA-CMP9 Modified Collagen Gel. To investigate the potential of our VEGF/**PA-CMP9**/collagen gel system to stimulate microvessel formation, HUVECs (passage 6) were added to VEGF/**PA-CMP9**-modified collagen gel. We prepared a type I collagen gel (200 μL of total volume) in a 48-well culture plate by neutralizing and warming cold acid soluble collagen solution as described above. To the gel was added 100 μL of **PA-CMP** solution (**hPA-CMP9** or **qPA-CMP9**) and the resulting gel was washed with 4 °C PBS.

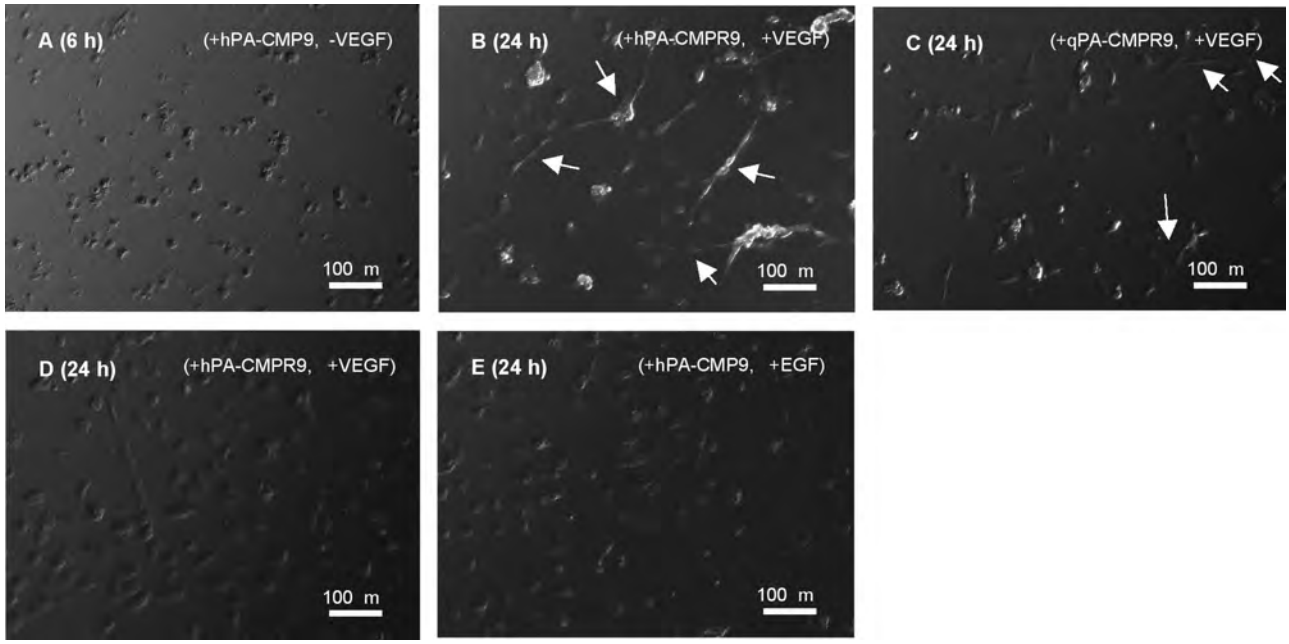

Figure 4. Optical micrographs of type I collagen gel treated with **hPA-CMP9** (A); **hPA-CMP9**/VEGF (B); **qPA-CMP9**/VEGF (C); **hPA-CMPR9**/VEGF (D); or **hPA-CMP9**/EGF (E) followed by HUVEC seeding and incubation at 37 °C for 6 or 24 h.

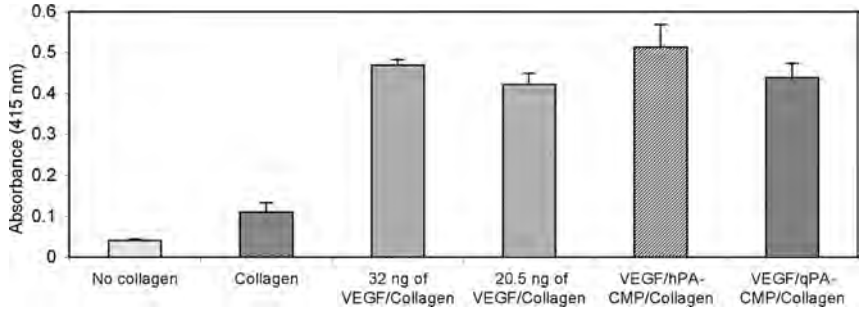

Figure 5. ILK assay that shows the bioactivity of VEGF in **PA-CMP9**/collagen gel. HUVECs (passage 6) were cultured 20 h before VEGF stimulation and the cells were incubated in EGM at 37 °C. Data are expressed as the mean ± SD.

After extensive cold wash, 100 μL of rhVEGF$_{165}$ solution (1 μg/mL) in PBS was added to the gel, and the gel was washed again with 4 °C PBS. In an effort to study the effect of VEGF immobilization, basic endothelial cell medium (EGM) without VEGF and with low-serum content were used for the culture, and EC's morphological changes were observed for only up to 24 h. Two control samples were also prepared; a collagen gel treated with **hPA-CMP9** but without VEGF addition (+**hPA-CMP9**, −VEGF) and a collagen gel treated with scrambled peptide **hPA-CMPR9** and VEGF (+**hPA-CMPR9**, +VEGF). Little cell attachment and spreading was observed when collagen gel was treated only with **hPA-CMP9** (Figure 4A), perhaps due to the high concentration of negative charges on collagen surfaces. Such cell repelling activity of anionically charged surfaces have been reported for patterned cell coculture studies and for surfaces modified to suppress immune response in medical implants.[49,50] Figure 4B,C shows the micrographs of the collagen gels treated with **hPA-CMP9** and **qPA-CMP9** 24 h after VEGF addition and HUVEC seeding. After 6 h of incubation, elongated morphology and cell−cell connections were readily observed (data not shown) and by 24 h, ECs showed signs of multicellular connections of long and narrow tube-like morphology (arrows). **hPA-CMP9** treatment produced higher level of tube-like morphology compared to **qPA-CMP9**, likely because of higher level of **PA-CMP9** and VEGF bound to the collagen gel. In contrast, under identical experimental conditions, the collagen gel treated with scrambled peptide, **hPA-CMPR9** and VEGF showed no signs of tube-like morphology (Figure 4D).

Although HUVEC morphology clearly demonstrated an enhanced thread-like transformation for **PA-CMP9** treated collagen gel in the presence of VEGF, it is possible that the tube-like morphology was caused by mechanism that is not mediated by VEGF but rather by the surface charges or other effects related to **PA-CMP9**. To address this concern, we performed a negative control experiment where epidermal growth factor (EGF) was used in place of VEGF. Similar to VEGF, EGF binds to negatively-charged molecules and can, therefore, neutralize the surface charges; however, EGF alone cannot induce tube-like morphology of ECs.[51−53] EGF treatment of **PA-CMP9**-modified collagen gel induced little tube-like morphology of ECs after a 1 day incubation (Figure 4E), confirming that the EC's morphological change was caused by a VEGF-specific mechanism.

We believe that the collagen-bound VEGF may be mimicking the angiogenic activity of VEGF$_{189}$ known to bind strongly to heparin of natural ECM. In a typical tubulogenesis assay where ECs are seeded on the surface of collagen gel in the presence of soluble VEGF, cells form a near-confluent layer on collagen gel before invading the matrix with elongated tube-like morphology; migration/differentiation of ECs typically takes place

after cells proliferate and contact each other. In our experiments, the cells seem to form thread-like structures even at relatively low cell density. They appear to be actively reaching out to make cell-cell connections despite the fair distance between the cells. After studying blood vessel morphogenesis of genetically engineered mouse embryos, Ruhrberg and co-workers concluded that soluble isoform of VEGF, $VEGF_{121}$, promotes EC proliferation and enlargement of existing blood vessels while matrix-bound isoform $VEGF_{189}$ promotes cell migration and new vessel formation.[16,19] In our experiment, HUVECs were seeded on **hPA-CMP9**-treated collagen gel with 30 ng of $VEGF_{165}$ bound to the collagen matrix (matrix volume, 200 μL; media volume, 500 μL). During a 24 h incubation at 37 °C, approximately 18 ng of the VEGF gradually dissociated from the matrix (Figure 3). These amounts correspond to 150 and 0 ng/mL of collagen-bound and soluble VEGF, respectively, at the time of cell seeding, and 60 and 18 ng/mL of collagen-bound and soluble VEGF, respectively, after 24 h of cell culture. Although the exact mechanism is unknown at this point, it seems that the high concentrations of collagen-bound VEGF played a critical role in the early morphological changes of the ECs. We are currently conducting long-term tubulogenesis experiment with ECs encapsulated inside the collagen gel, combined with morphological characterization that can identify lumen formation.

Integrin-Link Kinase (ILK) Assay for Determining VEGF Bioactivity in PA-CMP/ Collagen Gel System. We next performed an ILK assay that quantifies the VEGF-activated angiogenic pathway for both hot and quenched **PA-CMP9**/VEGF/collagen systems. Angiogenesis modulated by VEGF is significantly integrin-link kinase (ILK) dependent;[54−59] VEGF, an endothelial cell-specific mitogen has been shown to induce phosphatidylinositol 3-kinase (PI 3-kinase) activity by binding to vascular endothelial growth factor receptors (VEGFRs) on ECs.[60] Protein kinase B (PKB)/Akt is then activated in a complex manner through phosphorylation of Ser473.[56] To verify the biological activity of VEGF associated with **PA-CMP9**/collagen gel, we investigated whether the VEGF was able to activate this pathway in the HUVECs. The ILK assay was conducted on HUVECs cultured in **PA-CMP9**/VEGF/collagen and was compared to cells cultured in controlled conditions: culture dish only, pure collagen or collagen gel containing either 32 or 20.5 ng of soluble VEGF, which corresponds, respectively, to the initial concentrations of VEGF in **hPA-CMP9**/collagen and **qPA-CMP9**/collagen (day 0 in Figure 3B).

The ILK assay results are presented in Figure 5. ILK activation was relatively low for HUVECs cultured on dish only and pure collagen but increased by approximately 4−5-fold when the cells were cultured on VEGF containing collagen gel. When the assay was conducted on cells cultured in VEGF/**PA-CMP9**/collagen, the level of ILK activation was also high and nearly identical to that of the collagen gel treated with soluble VEGF; in fact, the levels of ILK activation for the heated and quenched system were both on par with those of HUVECs treated with the corresponding amount of soluble VEGF (32 ng for **hPA-CMP9** and 20.5 ng for **qPA-CMP9**). From the ILK assay results, we can safely conclude that the enhancement of HUVEC morphogenesis in VEGF/**PA-CMP9**/collagen systems is the result of biologically relevant VEGF-VEGF receptor activation pathway and not of unexpected and serendipitous effects of **PA-CMP9**.

Conclusions

In this report, we presented the synthesis and triple helical folding behavior of a new CMP architecture that bears multiple negative charges on its N-terminus designed to attract VEGF by charge−charge interaction. This CMP binds to type I collagen at room temperature and discharges from collagen at a sustained rate under physiological temperature as have been previously reported for other CMPs and CMP−poly(ethylene glycol) conjugates. When applied to 3D collagen gel (type I, bovine), the anionic CMPs promoted immobilization and sustained release of VEGF that resulted in enhanced tube-like morphology for HUVEC indicative of tubulogenesis. We believe that the negatively charged CMP can be applied to engineering both soft and hard tissues by immobilization of other growth factors (e.g., EGF) and inorganics (e.g., hydroxyapatite) that are known to bind to negatively charged biopolymers in ECM.[61]

Acknowledgment. We thank Professor Ernesto Freire for access to circular dichroism spectrometer and Dr. Xue Han for help with automated peptide synthesis. This work was supported by grants from the National Institute of Health (R21GM-74812) and National Science Foundation (DMR-0645411) to S.M.Y.

References and Notes

(1) Ennett, A. B.; Mooney, D. J. *Expert Opin. Biol. Ther.* **2002**, *2*, 805–818.
(2) Koike, N.; Fukumura, D.; Gralla, O.; Au, P.; Schechner, J. S.; Jain, R. K. *Nature* **2004**, *428*, 138–139.
(3) McGuire, B. J.; Secomb, T. W. *Am. J. Physiol. Heart Circ. Physiol.* **2003**, *285*, H2382–2391.
(4) Ingber, D.; Folkman, J. *Lab. Invest.* **1988**, *59*, 44–51.
(5) Wissink, M. J.; Beernink, R.; Pieper, J. S.; Poot, A. A.; Engbers, G. H.; Beugeling, T.; van Aken, W. G.; Feijen, J. *Biomaterials* **2001**, *22*, 151–163.
(6) Wissink, M. J.; Beernink, R.; Poot, A. A.; Engbers, G. H.; Beugeling, T.; van Aken, W. G.; Feijen, J. *J. Controlled Release* **2000**, *64*, 103–114.
(7) Kaihara, S.; Borenstein, J.; Koka, R.; Lalan, S.; Ochoa, E. R.; Ravens, M.; Pien, H.; Cunningham, B.; Vacanti, J. P. *Tissue Eng.* **2000**, *6*, 105–117.
(8) Sieminski, A. L.; Gooch, K. J. *Biomaterials* **2000**, *21*, 2232–2241.
(9) Carmeliet, P.; Jain, R. K. *Nature* **2000**, *407*, 249–257.
(10) Folkman, J.; Haudenschild, C. *Nature* **1980**, *288*, 551–556.
(11) Jain, R. K.; Schlenger, K.; Hockel, M.; Yuan, F. *Nat. Med.* **1997**, *3*, 1203–1208.
(12) Ucuzian, A. A.; Greisler, H. P. *World J. Surg.* **2007**, *31*, 654–663.
(13) Coultas, L.; Chawengsaksophak, K.; Rossant, J. *Nature* **2005**, *438*, 937–945.
(14) Ferrara, N.; Gerber, H. P.; LeCouter, J. *Nat. Med.* **2003**, *9*, 669–676.
(15) Shima, D. T.; Kuroki, M.; Deutsch, U.; Ng, Y. S.; Adamis, A. P.; D'Amore, P. A. *J. Biol. Chem.* **1996**, *271*, 3877–3883.
(16) Ruhrberg, C.; Gerhardt, H.; Golding, M.; Watson, R.; Ioannidou, S.; Fujisawa, H.; Betsholtz, C.; Shima, D. T. *Genes Dev.* **2002**, *16*, 2684–2698.
(17) Houck, K. A.; Leung, D. W.; Rowland, A. M.; Winer, J.; Ferrara, N. *J. Biol. Chem.* **1992**, *267*, 26031–26037.
(18) Park, J. E.; Keller, G. A.; Ferrara, N. *Mol. Biol. Cell* **1993**, *4*, 1317–1326.
(19) Ruhrberg, C. *Bioessays* **2003**, *25*, 1052–1060.
(20) Ennett, A. B.; Kaigler, D.; Mooney, D. J. *J. Biomed. Mater. Res.* **2006**, *79A*, 176–184.
(21) Fischbach, C.; Mooney, D. J. *Biomaterials* **2007**, *28*, 2069–2076.
(22) Leach, J. K.; Kaigler, D.; Wang, Z.; Krebsbach, P. H.; Mooney, D. J. *Biomaterials* **2006**, *27*, 3249–3255.
(23) Silva, E. A.; Mooney, D. J. *J. Thromb. Haemost.* **2007**, *5*, 590–598.
(24) Crombez, M.; Chevallier, P.; Gaudreault, R. C.; Petitclerc, E.; Mantovani, D.; Laroche, G. *Biomaterials* **2005**, *26*, 7402–7409.
(25) Seliktar, D.; Zisch, A. H.; Lutolf, M. P.; Wrana, J. L.; Hubbell, J. A. *J. Biomed. Mater. Res.* **2004**, *68A*, 704–716.
(26) Zisch, A. H.; Lutolf, M. P.; Ehrbar, M.; Raeber, G. P.; Rizzi, S. C.; Davies, N.; Schmokel, H.; Bezuidenhout, D.; Djonov, V.; Zilla, P.; Hubbell, J. A. *FASEB J.* **2003**, *17*, 2260–2262.
(27) Francis, M. E.; Uriel, S.; Brey, E. M. *Tissue Eng.* **2007**, *14B*, 19–32.
(28) Lee, C. H.; Singla, A.; Lee, Y. *Int. J. Pharm.* **2001**, *221*, 1–22.
(29) Yannas, I. V. *Angew. Chem., Int. Ed.* **1990**, *29*, 20–35.
(30) Sano, A.; Hojo, T.; Maeda, M.; Fujioka, K. *Adv. Drug Delivery Rev.* **1998**, *31*, 247–266.

(31) Ellis, D. L.; Yannas, I. V. *Biomaterials* **1996**, *17*, 291–299.
(32) Pieper, J. S.; Hafmans, T.; Veerkamp, J. H.; van Kuppevelt, T. H. *Biomaterials* **2000**, *21*, 581–593.
(33) Pieper, J. S.; van Wachem, P. B.; van Luyn, M. J. A.; Brouwer, L. A.; Hafmans, T.; Veerkamp, J. H.; van Kuppevelt, T. H. *Biomaterials* **2000**, *21*, 1689–1699.
(34) Ishikawa, T.; Eguchi, M.; Wada, M.; Iwami, Y.; Tono, K.; Iwaguro, H.; Tamaki, T.; Asahara, T. *Arterioscler., Thromb., Vasc. Biol.* **2006**, *26*, 1998–2004.
(35) Koch, S.; Yao, C.; Grieb, G.; Prevel, P.; Noah, E. M.; Steffens, G. C. *J. Mater. Sci.: Mater. Med.* **2006**, *17*, 735–741.
(36) Dong, C.-M.; Wu, X.; Caves, J.; Rele, S. S.; Thomas, B. S.; Chaikof, E. L. *Biomaterials* **2005**, *26*, 4041–4049.
(37) Wang, A. Y.; Mo, X.; Chen, C. S.; Yu, S. M. *J. Am. Chem. Soc.* **2005**, *127*, 4130–4131.
(38) Nimni, M. E.; Olsen, B. R.; Kang, A. H. *Collagen*; CRC Press: Boca Raton, FL, 1988.
(39) Khoshnoodi, J.; Cartailler, J. P.; Alvares, K.; Veis, A.; Hudson, B. G. *J. Biol. Chem.* **2006**, *281*, 38117–38121.
(40) Mo, X.; An, Y. J.; Yun, C. S.; Yu, S. M. *Angew. Chem., Int. Ed.* **2006**, *45*, 2267–2270.
(41) Lee, J. H.; Yu, C.; Chansakul, T.; Hwang, N. S.; Varghese, S.; Yu, S. M.; Elisseeff, J. H. *Tissue Eng.* **2008**,
(42) Lee, J. H.; Lee, J. S.; Chansakul, T.; Yu, C.; Elisseeff, J. H.; Yu, S. M. *Biomaterials* **2006**, *27*, 5268–5276.
(43) Kantchev, E. A. B.; Chang, C.-C.; Chang, D.-K. *Biopolymers* **2006**, *84*, 232–240.
(44) Bretscher, L. E.; Jenkins, C. L.; Taylor, K. M.; DeRider, M. L.; Raines, R. T. *J. Am. Chem. Soc.* **2001**, *123*, 777–778.
(45) Holmgren, S. K.; Bretscher, L. E.; Taylor, K. M.; Raines, R. T. *Chem. Biol.* **1999**, *6*, 63–70.
(46) Clark, M. F.; Adams, A. N. *J. Gen. Virol.* **1977**, *34*, 475–483.
(47) Kotch, F. W.; Raines, R. T. *Proc. Natl. Acad. Sci. U.S.A.* **2006**, *103*, 3028–3033.
(48) Wang, A. Y.; Foss, C. A.; Leong, S.; Mo, X.; Pomper, M. G.; Yu, S. M. *Biomacromolecules* **2008**, *9*, 1755–1763.
(49) Brodbeck, W. G.; Patel, J.; Voskerician, G.; Christenson, E.; Shive, M. S.; Nakayama, Y.; Matsuda, T.; Ziats, N. P.; Anderson, J. M. *Proc. Natl. Acad. Sci. U.S.A.* **2002**, *99*, 10287–10292.
(50) Kaji, H.; Sekine, S.; Hashimoto, M.; Kawashima, T.; Nishizawa, M. *Biotechnol. Bioeng.* **2007**, *98*, 919–925.
(51) Chen, C. S.; Mrksich, M.; Huang, S.; Whitesides, G. M.; Ingber, D. E. *Science* **1997**, *276*, 1425–1428.
(52) Miura, M.; Fujimoto, K. *Colloids Surf., B* **2006**, *53*, 245–153.
(53) Takehara, K.; LeRoy, E. C.; Grotendorst, G. R. *Cell* **1987**, *49*, 415–422.
(54) Ariedrich, E. B.; Liu, E.; Sinha, S.; Cook, S.; Milstone, D. S.; MacRae, C. A.; Mariotti, M.; Kuhlencordt, P. L.; Force, T.; Rosenzweig, A.; St-Arnaud, R.; Dedhar, S.; Gerszten, R. E. *Mol. Cell. Biol.* **2004**, *24*, 8134–8144.
(55) Hannigan, G.; Troussard, A. A.; Dedhar, S. *Nat. Rev. Cancer* **2005**, *5*, 51–63.
(56) Kaneko, Y.; Kitazato, K.; Basaki, Y. *J. Cell Sci.* **2004**, *117*, 407–415.
(57) Koul, D.; Shen, R.; Bergh, S.; Lu, Y.; de Groot, J. F.; Liu, T. J.; Mills, G. B.; Yung, W. K. *Mol. Cancer Ther.* **2005**, *4*, 1681–1688.
(58) Tan, C.; Cruet-Hennequart, S.; Troussard, A.; Fazli, L.; Costello, P.; Sutton, K.; Wheeler, J.; Gleave, M.; Sanghera, J.; Dedhar, S. *Cancer Cell* **2004**, *5*, 79–90.
(59) Watanabe, M.; Fujioka-Kaneko, Y.; Kobayashi, H.; Kiniwa, M.; Kuwano, M.; Basaki, Y. *Biol. Proced. Online* **2005**, *7*, 41–47.
(60) Kevil, C. G.; Payne, D. K.; Mire, E.; Alexander, J. S. *J. Biol. Chem.* **1998**, *273*, 15099–15103.
(61) Sarvestani, A. S.; He, X.; Jabbari, E. *Biopolymers* **2007**, *85*, 370–378.

BM800727Z